Nanoparticles

DOI: 10.1002/anie.201308843

Near-Infrared-Light-Mediated Imaging of Latent Fingerprints based on Molecular Recognition**

*Jie Wang, Ting Wei, Xinyang Li, Binhao Zhang, Jiaxi Wang, Chi Huang, and Quan Yuan**

Abstract: *Photoluminescence is one of the most sensitive techniques for fingerprint detection, but it also suffers from background fluorescence and selectivity at the expense of generality. The method described herein integrates the advantages of near-infrared-light-mediated imaging and molecular recognition. In principle, upconversion nanoparticles (UCNPs) functionalized with a lysozyme-binding aptamer were used to detect fingerprints through recognizing lysozyme in the fingerprint ridges. UCNPs possess the ability to suppress background fluorescence and make it possible for fingerprint imaging on problematic surfaces. Lysozyme, a universal compound in fingerprints, was chosen as the target, thus simultaneously meeting the selectivity and generality criteria in photoluminescence approaches. Fingerprints on different surfaces and from different people were detected successfully. This strategy was used to detect fingerprints with cocaine powder by using UCNPs functionalized with a cocaine-binding aptamer.*

Fingerprints have long been utilized as one of the most useful types of physical evidence and have found wide applications in areas such as forensic investigations, access control, and medical diagnostics.[1] Some fingerprints are visible if the fingers are contaminated with blood or paint, and latent fingerprints are invisible to the bare eye.[2] The basic principle of latent-fingerprint detection is the generation of an optical contrast between the ridges of the fingerprint and the affected surface.[3] Until now, various techniques have been developed for fingerprint imaging. Li et al. reported a sensitive technique by using nanoplasmonic technology for latent-fingerprint detection.[4] Su et al. developed a novel two-step method for fingerprint detection by electrochemiluminescence, and put forward a new pathway to nondestructive analysis.[5] Among all the existing detection techniques,[6] photoluminescence has led to new levels of sensitivity.[7] Usually, the photoluminescence technique involves a luminescent material conjugated to a reagent which selectively attacks a component of the fingerprint residue. Despite the advantages of this technique, it still suffers from two major drawbacks: background fluorescence[8] and selectivity at the expense of generality.[1] Although techniques such as time-resolved photoluminescence imaging have been developed to suppress the background fluorescence, these techniques often involve expensive instrumentation. In addition, the reagents currently used usually bind to exogenous compounds doped in fingerprints, thus greatly limiting photoluminescence as a general approach. As a consequence, there is a strong need to develop a general strategy for latent-fingerprint detection with high selectivity and suppressed background fluorescence. Herein, we have combined upconversion nanomaterials with a DNA aptamer to target a universal compound in fingerprints and provide a general and easily performed strategy for latent-fingerprint imaging under near-infrared (NIR) light excitation. This approach can be applied to fingerprints on different surfaces and from different people, without any interference from background fluorescence.

To remedy the interference of background fluorescence from the surface, luminescence materials that can suppress the background fluorescence hold great potential. Upconversion nanoparticles (UCNPs), particularly lanthanide-doped rare-earth nanocrystals, are believed to be the key to the next generation of imaging.[9] Through sequential electronic excitation and energy-transfer processes, UCNPs are capable of converting two or more NIR pump photons into a higher-energy output photon.[10] Because fluorophores in various substrates cannot be excited by NIR light, the imaging of latent fingerprints with UCNPs suffers little from background fluorescence interference, thus offering excellent optical contrast and allowing high detection sensitivity.[11] In addition, UCNPs have excellent properties, such as exceptional photostability, fine-tuned emissions, high quantum yields, and long lifetimes, which endow these nanoparticles with many advantages over other fluorescence reagents.[12] Given these properties, UCNPs are ideal candidates for latent-fingerprint imaging.

To simultaneously meet the selectivity and generality criteria for photoluminescence detection, it is necessary to target a compound that is universal in fingerprints. Previous research has shown that lysozyme is one of the polypeptide components in human sweat.[13] Thus, lysozyme from the hands can serve as a universal target in fingerprints for photoluminescence approaches. In recent years, single-stranded DNA or RNA, called aptamers, have attracted much attention for the recognition of molecules of interest with high selectivity and affinity.[14] Aptamers have emerged as appealing biomolecules that rival antibodies in detection, targeted imaging, and diagnostic applications.[15] Compared with antibodies, aptamers display many exceptional properties, such as design flexibility, tolerant of harsh synthetic

[*] J. Wang, T. Wei, X. Li, B. Zhang, J. Wang, C. Huang, Prof. Dr. Q. Yuan
Key Laboratory of Analytical Chemistry for Biology and Medicine (Ministry of Education), College of Chemistry and Molecular Sciences, Wuhan University, Wuhan 430072 (China)
E-mail: yuanquan@whu.edu.cn

[**] This work was supported by the National Natural Science Foundation of China (21201133, 51272186). Q.Y. thanks Wuhan University for start-up funds and the large-scale instrument and equipment sharing foundation of Wuhan University.

Supporting information for this article is available on the WWW under http://dx.doi.org/10.1002/anie.201308843.

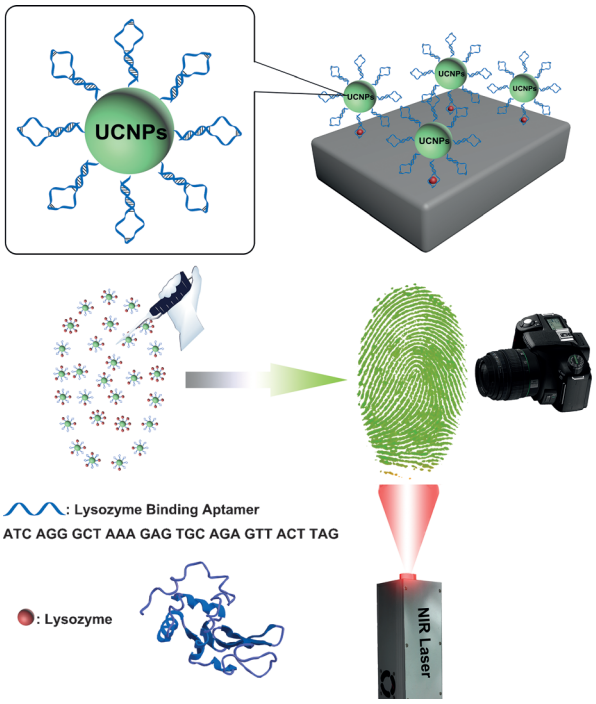

Scheme 1. Strategy for latent-fingerprint detection with UCNPs functionalized with a lysozyme-binding aptamer nanoconjugates.

conditions, easy modification, and biochemical stability.[16] Cox et al. reported a DNA aptamer targeting lysozyme, and their interaction has been extensively studied.[17] Therefore, a lysozyme-binding aptamer (designated as LBA) was chosen as a general targeting reagent for latent fingerprints.

The design principle is outlined in Scheme 1. UCNPs were functionalized with LBA (designated as UCNPs-LBA) by amide-bond formation. Lysozyme, serving as a universal target in fingerprint ridges, leads to the deposition of UCNPs-LBA on the ridges after recognition by the nanoconjugate. When UCNPs-LBA were excited by a portable NIR laser with emission at $\lambda = 980$ nm, no background fluorescence was observed. Because of the simplicity of this strategy, a standard digital single-lens reflex camera equipped with a macro lens was all that was necessary for capturing the images of fingerprints. The above process can be easily performed since no complicated or expensive instrumentation was involved. We also investigated the feasibility of this design for exogenous compound detection in latent fingerprints. A cocaine-binding aptamer (CBA) was conjugated with UCNPs (UCNPs-CBA) for detection of cocaine in fingerprints and provided images of high evidential quality with resolution sufficient for identification of the individual as well as the drug. Our design may shed new light on latent-fingerprint imaging as a general and easily performed photoluminescence detection strategy.

$NaYF_4$ UCNPs doped with 20% Yb and 2% Er ($NaYF_4$:20% Yb, 2% Er) were synthesized using a previously reported protocol.[18] The representative transmission-electron microscopy (TEM) images of the as prepared UCNPs showed that the nanoparticles had well-defined hexagonal shapes with an average diameter of 260 nm (see Figure S1 in the Supporting Information). Figure 1a shows the functionalization steps for constructing the UCNPs-LBA. First, UCNPs were capped with a layer of oleic acid (designated as OA-UCNPs) for use as a surfactant and capping ligands in the synthesis process. For further conjugation, OA-UCNPs were modified with poly(acrylic acid) (designated as PAA-UCNPs) by a ligand-exchange procedure, which introduced carboxy functional groups for connection with biologically active molecules.[19] Finally, PAA-UCNPs were linked with amino-group-labeled LBA (designated as LAB-NH_2) to form the UCNPs-LBA nanoconjugates. The obtained UCNPs-LBA exhibited uniform hexagonal shapes, as shown in Figure 1b. Energy-dispersive X-ray (EDX) analysis of UCNPs-LBA demonstrated the existence of Y, Yb, and Er in the nanoconjugate (Figure 1c). The upconversion luminescent feature of UCNPs-LBA was measured by excitation with an NIR laser (Figure 1d), and the results were similar to those of OA-UCNPs and PAA-UCNPs (see Figure S6). The inset in Figure 1d indicates that UCNPs-LBA have excellent water solubility, with luminescence predominantly green in color upon excitation at $\lambda = 980$ nm. The functionalization steps were verified by FT-IR spectroscopy, as shown in Figure 1e. For OA-UCNPs, the two bands at around 1562 cm^{-1} and 1461 cm^{-1} correspond to the in-plane bending vibration of =C–H in the OA molecule. After PAA modification, PAA-UCNPs showed the characteristic stretching vibrations of the

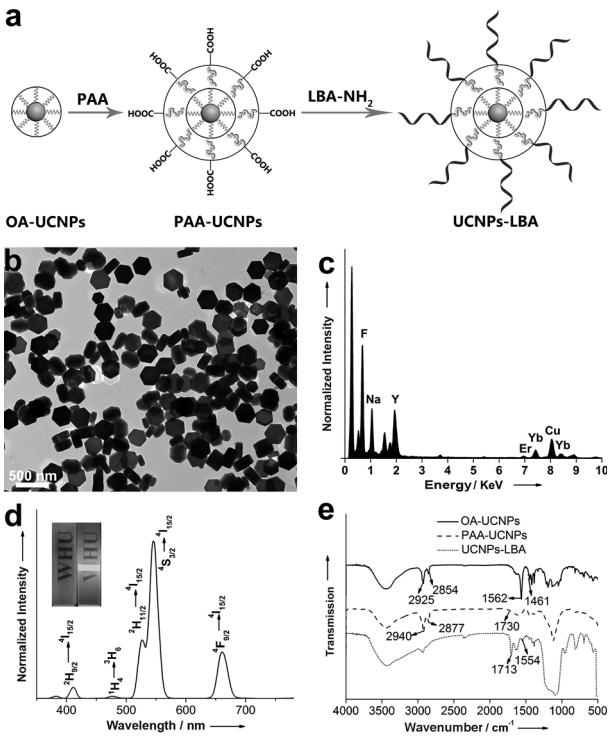

Figure 1. a) Functionalization steps to construct the UCNPs functionalized with a lysozyme-binding aptamer (UCNPs-LBA). b) TEM images of the as-prepared UCNPs-LBA. c) EDX analysis of UCNPs-LBA. d) Upconversion luminescence spectra of UCNPs-LBA. Inset: Corresponding luminescence photographs of UCNPs-LBA under excitation with an NIR laser. e) FTIR absorption spectra of oleic acid stabilized UCNPs (OA-UCNPs), poly(acrylic acid) stabilized UCNPs (PAA-UCNPs), and UCNPs-LBA.

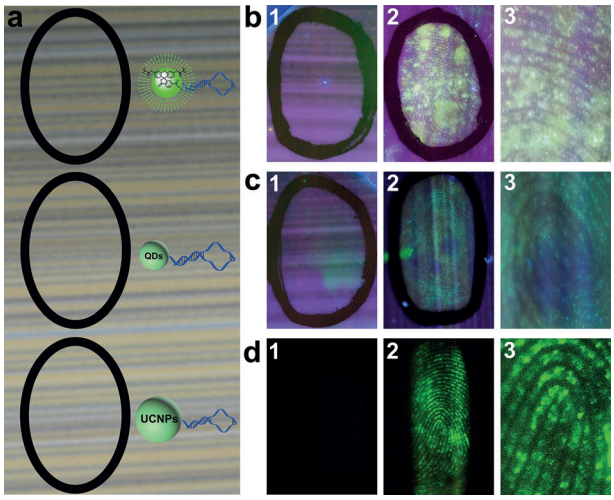

Figure 2. a) Photograph of the marble with three latent fingerprints in the black circles. Inset: FAM-labeled lysozyme-binding aptamer, and QDs and UCNPs functionalized with a lysozyme-binding aptamer. b) Luminescence image of fingerprints treated with FAM solution (1), FAM-LBA (2), and the corresponding magnified image (3). c) Luminescence image of fingerprints treated with QDs solution (1), QDs-LBA (2), and the corresponding magnified image (3). d) Luminescence image of fingerprints treated with PAA-UCNPs (1), UCNPs-LBA (2), and the corresponding magnified image (3).

C=O bond at 1730 cm^{-1}. The UCNPs-LBA nanoconjugates displayed two vibrational peaks at around 1713 cm^{-1} and 1554 cm^{-1}, which are attributed to the asymmetric stretching mode of the imidoyl group and the amide vibrations. In addition, the above functionalization steps were further confirmed by zeta potential and UV/Vis absorption measurements. As shown in Figure S3, PAA-UCNPs were negatively charged (−12.0 mV) because of the carboxy group in PAA, and UCNPs-LBA had a greater negative charge of −31.1 mV, which is attributed to the phosphate groups in the DNA backbone. In the UV/Vis spectra (Figure S4), UCNPs-LBA showed a typical absorption at $\lambda = 260$ nm, thus indicating the successful conjugation of LBA to the nanoparticles.

The performance of UCNPs-LBA for latent-fingerprint detection was tested on a household marble surface which was used daily (Figure 2a). In addition, fluorescein amidite (FAM) and CdTe quantum dots (QDs) were used to image fingerprints. FAM-labeled LBA (designated as FAM-LBA) showed strong emission at around $\lambda = 520$ nm (Figure S7). CdTe QDs with emission at around $\lambda = 540$ nm were capped with a layer of L-cysteine and additionally conjugated with LBA-NH_2 (QDs-LBA). As shown in Figure 2b1, no fingerprint images were obtained after incubation with FAM solution only, and the marble showed strong purple fluorescence under excitation with light of $\lambda = 365$ nm. Figure 2b2 shows the fluorescence image of fingerprints recorded by a digital single-lens reflex camera equipped with a macro lens after incubation with FAM-LBA solution, and a higher magnification image is shown in Figure 2b3. From these two figures, we can clearly see the strong interference from the background fluorescence of the marble, thus making it difficult to identify ridged patterns and greatly affecting the imaging sensitivity. Figure 2c shows the fluorescence image of fingerprints imaged with QDs and the images were also strongly impaired by the background fluorescence. When it came to fingerprints imaged with UCNPs (Figure 2d), much better results were obtained. Fingerprints treated with PAA-UCNPs solution did not form a luminescence image (Figure 2d1), thus indicating that UCNPs without LBA cannot bind to the fingerprints. Most importantly, the marble surface did not show any fluorescence under NIR light irradiation, thus revealing the ability of UCNPs to suppress background fluorescence. Figure 2d2 shows a clear luminescence image without any interference from background fluorescence after incubation with a UCNPs-LBA solution. At higher magnifications (Figure 2d3), specific details of the fingerprint pattern, such as arches and termination points, can be easily recognized. Accordingly, one can safely draw the conclusion that UCNPs-LBA not only suppress the background fluorescence interference, but also bind to fingerprints through the recognition of lysozyme in the ridges, thus demonstrating the great potential of UCNPs-LBA nanoconjugates for latent-fingerprint imaging.

In addition, we determined the applicability of UCNPs-LBA nanoconjugates on different surfaces. A fingerprint on a smooth glass microscope slide (Figure 3a) was treated with UCNPs-LBA solution. It showed a clear and bright luminescence image (Figure 3b1) under excitation with NIR light, and the ridge pattern details could be easily recognized at higher magnification (Figure 3b2). Compared to smooth surfaces, fingerprints on semiporous substrates such as plastics are usually more difficult to detect. A similar

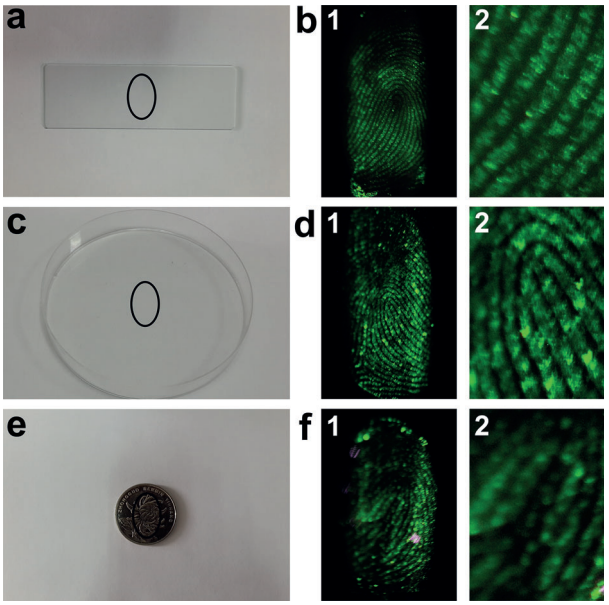

Figure 3. a) Photograph of a glass microscope slide with a latent fingerprint in the black circle. b) Luminescence image of fingerprint on the slide (1) and the corresponding magnified image (2). c) Photograph of a Petri dish with a latent fingerprint in the black circle. d) Luminescence image of fingerprint on Petri dish (1) and the corresponding magnified image (2). e) Photograph of a patterned coin with a latent fingerprint in the black circle. f) Luminescence image of fingerprint on the coin (1) and the corresponding magnified image (2).

experiment was performed for fingerprints on a plastic Petri dish (Figure 3c), and clear luminescence images of fingerprint ridges can be easily recognized (Figure 3d1 and d2). Additionally, a patterned coin (Figure 3e) was used as the surface for fingerprints and the resulting images of fingerprints treated with UCNPs-LBA are shown in Figure 3f. Similar to the former two cases, clear luminescence images of fingerprint were obtained (Figure 3f1 and f2), thus indicating the ability of UCNPs-LBA to eliminate the surface pattern. It is noteworthy that none of the above images suffered from background fluorescence interference. We further investigated the applicability of this design by detecting fingerprints from different people. As shown in Figure S11, all of the luminescence images of fingerprints from ten volunteers displayed evident details of the typical ridge pattern which would provide useful evidence for individual identification. These observations clearly illustrate that this strategy can be applied successfully to fingerprints on different substrates and from different people, clearly demonstrating the good generality of this approach.

As mentioned above, we further expanded this strategy to cocaine detection in latent fingerprints. Figure 4a shows the schematic representation of the method used for investigating the interaction between cocaine and CBA. As shown in Figure 4b and Figure S14, the fluorescence of FAM-labeled CBA (FAM-CBA) was quenched by partially complementary black-hole-quencher-labeled single-strand DNA (cDNA-BHQ-1) after hybridization. Upon addition of cocaine, the fluorescence was recovered because of a competition reaction between cocaine and cDNA-BHQ-1. Fingerprints doped with different amounts of cocaine were incubated with UCNPs-CBA solution for half an hour. Figure 4c shows the image of a fingerprint without cocaine. No luminescence ridges were obtained after incubation, thus demonstrating that UCNPs-CBA cannot bind to the ridges of fingerprints without cocaine. Fingerprints doped with 10 μg of cocaine showed clear luminescence images (Figure 4d), and at higher magnifications (Figure 4e) significant details of the ridge pattern are clearly evident. When the doped amounts of cocaine were decreased to 5 μg and 1 μg (Figure 4f,g), clear luminescence images of fingerprints were also obtained. Figure 4h shows images of fingerprints doped with 0.1 μg of cocaine and ridges pattern can still be easily recognized. Furthermore, in this strategy CBA can also be replaced by other aptamers for detection of other exogenous substances in fingerprints, such as explosives. As a result, this flexible design can be applied to exogenous compound detection and simultaneously give clear images of fingerprints for individual identification, thus showing the potential to provide valuable information for forensic investigation.

In this work, we have combined the background fluorescence suppressing ability of UCNPs and the universality of lysozyme in fingerprints to construct a general and easily performed strategy for latent-fingerprint detection based on molecular recognition. This approach can be applied to fingerprints on different surfaces and from different people, thus indicating the great practicality of this method. By replacing LBA with CBA, fingerprints containing cocaine were detected successfully, and this design holds potential to be used for various kinds of exogenous substance detection by simply changing the type of aptamer. This strategy can serve as a robust approach for latent-fingerprint imaging, and we anticipate that this general method will find wide-ranging applications in forensic investigations and medical diagnostics.

Received: October 10, 2013
Revised: November 27, 2013
Published online: January 21, 2014

Keywords: aptamers · fluorescence · imaging agents · molecular recognition · nanoparticles

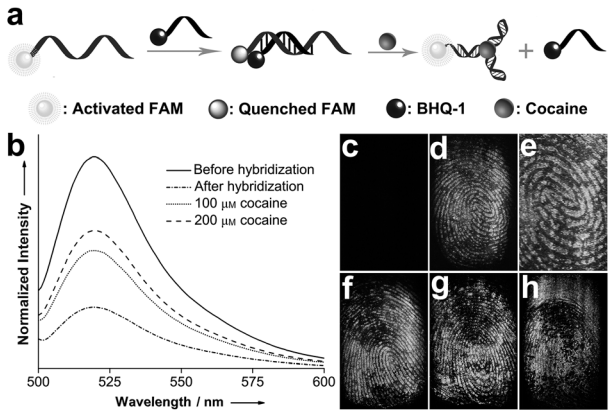

Figure 4. a) Interaction between a labeled cocaine-binding aptamer (CBA) and cocaine. b) Fluorescence spectra of FAM-labeled cocaine-binding aptamer (FAM-CBA) before and after hybridization with a partially complementary black-hole-quencher-labeled single-strand DNA (cDNA-BHQ-1; FAM-CBA/cDNA-BHQ-1, 1:1), and after addition of 100 μM and 200 μM of cocaine. c) Fingerprints without cocaine after incubation with UCNPs functionalized with a cocaine-binding aptamer. Luminescence image of fingerprints doped with 10 μg of cocaine (d) and the corresponding magnified image (e). Luminescence images of fingerprints doped with 5 μg (f), 1 μg (g) and 0.1 μg (h) of cocaine.

[1] M. Wood, P. Maynard, X. Spindler, C. Roux, C. Lennard, *Aust. J. Forensic Sci.* **2013**, *45*, 211 – 226.
[2] P. Hazarika, D. A. Russell, *Angew. Chem.* **2012**, *124*, 3582 – 3589; *Angew. Chem. Int. Ed.* **2012**, *51*, 3524 – 3531.
[3] A. Becue, S. Moret, C. Champod, P. Margot, *Biotech. Histochem.* **2011**, *86*, 140 – 160.
[4] K. Li, W. W. Qin, F. Li, X. C. Zhao, B. W. Jiang, K. Wang, S. H. Deng, C. H. Fan, D. Li, *Angew. Chem.* **2013**, *125*, 11756 – 11759; *Angew. Chem. Int. Ed.* **2013**, *52*, 11542 – 11545.
[5] L. R. Xu, Y. Li, S. Z. Wu, X. H. Liu, B. Su, *Angew. Chem.* **2012**, *124*, 8192 – 8196; *Angew. Chem. Int. Ed.* **2012**, *51*, 8068 – 8072.
[6] a) G. S. Sodhi, J. Kaur, *Forensic Sci. Int.* **2001**, *120*, 172 – 176; b) D. B. Hansen, M. M. Joullié, *Chem. Soc. Rev.* **2005**, *34*, 408 – 417; c) E. Stauffer, A. Becue, K. V. Singh, K. R. Thampi, C. Champod, P. Margot, *Forensic Sci. Int.* **2007**, *168*, e5 – e9; d) D. R. Ifa, N. E. Manicke, A. L. Dill, R. G. Cooks, *Science* **2008**, *321*, 805; e) J. S. Day, H. G. M. Edwards, S. A. Dobrowski, A. M. Voice, *Spectrochim. Acta Part A* **2004**, *60*, 1725 – 7130; f) X. N. Shan, U. Patel, S. P. Wang, R. Iglesias, N. J. Tao, *Science* **2010**, *327*, 1363 – 1366.
[7] a) A. Becue, A. Scoundrianos, C. Champod, P. Margot, *Forensic Sci. Int.* **2008**, *179*, 39 – 43; b) R. Leggett, E. E. Lee-Smith, S. M.

Jickells, D. A. Russell, *Angew. Chem.* **2007**, *119*, 4178 – 4181; *Angew. Chem. Int. Ed.* **2007**, *46*, 4100 – 4103; c) P. Hazarika, S. M. Jickells, K. Wolff, D. A. Russell, *Angew. Chem.* **2008**, *120*, 10321 – 10324; *Angew. Chem. Int. Ed.* **2008**, *47*, 10167 – 10170; d) P. Hazarika, S. M. Jickells, K. Wolff, D. A. Russell, *Anal. Chem.* **2010**, *82*, 9150 – 9154.

[8] a) P. Maynard, J. Jenkins, C. Edey, G. Payne, C. Lennard, A. McDonagh, C. Roux, *Aust. J. Forensic Sci.* **2009**, *41*, 43 – 62; b) M. Sametband, I. Shweky, U. Banin, D. Mandler, J. Almog, *Chem. Commun.* **2007**, 1142 – 1144; c) N. Akiba, N. Saitoh, K. Kuroki, N. Igarashi, K. Kurosawa, *J. Forensic Sci.* **2011**, *56*, 754 – 759.

[9] a) H. S. Mader, P. Kele, S. M. Saleh, O. S. Wolfbeis, *Curr. Opin. Chem. Biol.* **2010**, *14*, 582 – 596; b) L. Cheng, C. Wang, Z. Liu, *Nanoscale* **2013**, *5*, 23 – 37; c) J. Shen, L. Zhao, G. Han, *Adv. Drug Delivery Rev.* **2013**, *65*, 744 – 755.

[10] a) J. Zhou, Z. Liu, F. Li, *Chem. Soc. Rev.* **2012**, *41*, 1323 – 1349; b) M. Haase, H. Schäfer, *Angew. Chem.* **2011**, *123*, 5928 – 5950; *Angew. Chem. Int. Ed.* **2011**, *50*, 5808 – 5829; c) F. Wang, D. Banerjee, Y. S. Liu, X. Y. Chen, X. G. Liu, *Analyst* **2010**, *135*, 1839 – 1854.

[11] a) Y. Yang, Q. Zhao, W. Feng, F. Li, *Chem. Rev.* **2013**, *113*, 192 – 270; b) D. Tu, L. Liu, Q. Ju, Y. Liu, H. Zhu, R. Li, X. Chen, *Angew. Chem.* **2011**, *123*, 6430 – 6434; *Angew. Chem. Int. Ed.* **2011**, *50*, 6306 – 6310.

[12] a) L. L. Li, P. W. Wu, K. Hwang, Y. Lu, *J. Am. Chem. Soc.* **2013**, *135*, 2411 – 2414; b) Q. Ju, D. Tu, Y. Liu, R. Li, H. Zhu, J. Chen, Z. Chen, M. Huang, X. Chen, *J. Am. Chem. Soc.* **2012**, *134*, 1323 – 1330.

[13] a) V. L. Chen, D. S. France, G. P. Martinelli, *J. Invest. Dermatol.* **1986**, *87*, 585 – 587; b) B. Hartzell-Baguley, R. E. Hipp, N. R. Morgan, S. L. Morgan, *J. Chem. Educ.* **2007**, *84*, 689 – 691.

[14] a) W. H. Tan, M. J. Donovan, J. H. Jiang, *Chem. Rev.* **2013**, *113*, 2842 – 2862; b) H. Xing, N. Y. Wong, Y. Xiang, Y. Lu, *Curr. Opin. Chem. Biol.* **2012**, *16*, 429 – 435.

[15] a) F. Gu, L. Zhang, B. A. Teply, N. Mann, A. Wang, A. F. R. Moreno, R. Langer, O. C. Farokhzad, *Proc. Natl. Acad. Sci. USA* **2008**, *105*, 2586 – 2591; b) N. L. Rosi, D. A. Giljohann, C. S. Thaxton, A. K. R. Lytton-Jean, M. S. Han, C. A. Mirkin, *Science* **2006**, *312*, 1027 – 1030; c) H. Liu, Y. Xiang, Y. Lu, R. M. Crooks, *Angew. Chem.* **2012**, *124*, 7031 – 7034; *Angew. Chem. Int. Ed.* **2012**, *51*, 6925 – 6928.

[16] a) X. Fang, W. Tan, *Acc. Chem. Res.* **2010**, *43*, 48 – 57; b) Z. Zhu, Z. Tang, J. A. Phillips, R. Yang, H. Wang, W. Tan, *J. Am. Chem. Soc.* **2008**, *130*, 10856 – 10857; c) Y. Du, B. Li, E. Wang, *Acc. Chem. Res.* **2013**, *46*, 203 – 213; d) J. Liu, Z. Cao, Y. Lu, *Chem. Rev.* **2009**, *109*, 1948 – 1998.

[17] a) J. C. Cox, A. D. Ellington, *Bioorg. Med. Chem.* **2001**, *9*, 2525 – 2531; b) M. Girardota, H. Y. Li, A. Varenne, *J. Chromatogr. A* **2011**, *1218*, 4052 – 4058.

[18] H. X. Mai, Y. W. Zhang, R. Si, Z. G. Yan, L. D. Sun, L. P. You, C. H. Yan, *J. Am. Chem. Soc.* **2006**, *128*, 6426 – 6436.

[19] L. Q. Xiong, T. S. Yang, Y. Yang, C. J. Xu, F. Y. Li, *Biomaterials* **2010**, *31*, 7078 – 7085.

